Predicting the Reactivity of Acyclic Silylenes and Germylenes in Hydrogen Activation

Michelle Kleinhaus[a] and Viktoria H. Gessner*[a]

Chair of Inorganic Chemistry II, Faculty of Chemistry and Biochemistry, Ruhr-University Bochum;
Universitätsstraße 150, 44801 Bochum
E-mail: viktoria. gessner@rub.de

Abstract. Divalent group 14 element compounds (heavier carbenes) have been shown to serve as transition metal mimics and thus can activate small molecules and strong bonds at mild reaction conditions. Incorporating this special ability into novel transition metal-free catalysts requires careful tuning of the molecular properties. Finding the optimal combination of substituents is challenging and an experimentally highly demanding process. In this work, we combine DFT and machine learning methods to predict the energy and activation barrier for the activation of dihydrogen by silylenes and germylenes, to thus facilitate the selection of candidates for small molecule activation in the future. We demonstrate that - based on the analysis of approx. 600 acyclic silylenes generated from 40 different substituents - the energy profiles can be reliably predicted by a simple model using the sum of energy increments of the substituents of the silylene. Furthermore, quantitative structure-activity relationships between the energies and the electronic and steric properties of the silylenes could be established, which enabled the prediction of the activation barrier with a mean average error of less than 9 kJ/mol. The model even enabled an extrapolation to silylenes with substituents not included in the original data set, and thus could predict new silylene structures for small molecule activation. Moreover, the reported procedure can also be applied to germylenes, and their energy profile quantitatively expressed as a function of the energies values of their silicon analogues. Overall, the presented protocol allows for a fast screening and prediction of possible candidates for H_2 activation, which will accelerate the development of main group element catalysts in the future.

Introduction

Low-valent main group compounds have long been considered as lab curiosities of limited stability and accessibility. However, research endeavors in the past three decades have changed this assumption and impressively demonstrated that species with most unusual bonding situations and electronic structures can be isolated and most importantly be applied in the activation of small molecules and strong bonds.[1] This has sparked interest in applying such compounds also in catalysis, with the prospect of developing sustainable, transition metal free alternatives to existing protocols. One of the most researched classes of low valent main group compounds applied in small molecule activation are carbenes and their heavier congeners, R-E-R' (E = C-Pb).[2] This interest was particularly fueled by the landmark report by Bertrand and coworkers in 2007 showing that alkyl(amino)carbenes (e.g. **B**, Figure 1) are

able to activate dihydrogen at mild temperatures, a transformation long thought to be exclusive to precious transition metals such as palladium, rhodium, iridium (e.g. **A**) or ruthenium.[3] This transition-metal like behavior is enabled by the availability of an energetically high lying lone pair in a non-bonding orbital and a low-lying vacant orbital at the group 14 element, a feature reminiscent of the often partially filled d-orbitals of the transition metals.

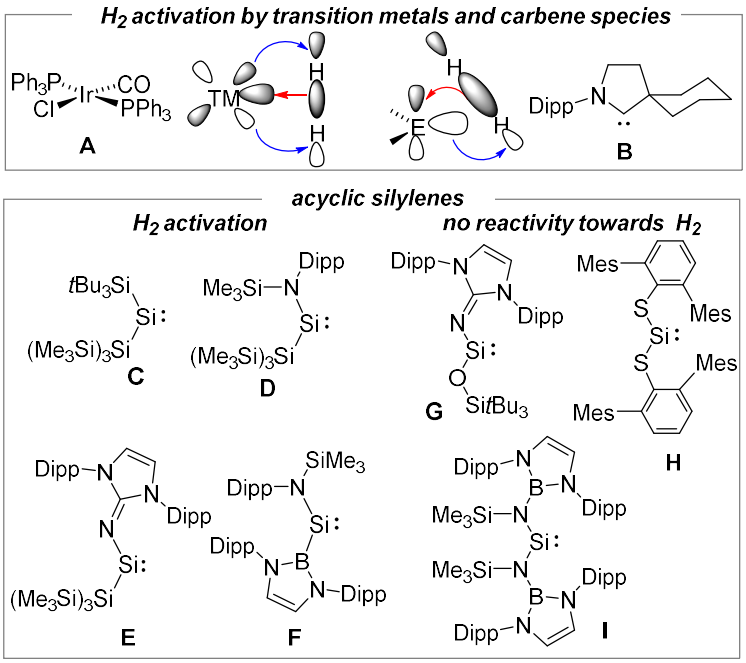

Figure 1. (Top) Dihydrogen activation at a transition metal and divalent group 14 element center; (Bottom) Examples of acyclic silylenes capable or incapable of activating dihydrogen.

With the motivation to substitute these transition metals in future hydrogenation reactions, vast research efforts have focused on the expansion of hydrogen activation to other carbenes as well as their heavier congeners. Investigations of the use of different substitution patterns and their impact on the H_2 activation capability led to a first understanding of the important electronic properties. For example, it has in general been accepted that a small HOMO-LUMO and small singlet-triplet energy gap enhance the activity of the divalent group 14 compounds towards bond activations.[3,4] Owing to the increased stability of the +2 oxidation state within the group, the activity decreases from carbon to lead. Thus, also several acyclic silylenes[5,6] and few germylenes[4d,7] have been reported to undergo H_2 activation at the group 14 element center (Figure 1). However, for establishing catalytic protocols not only the kinetic but also the thermodynamic profile for H_2 activation needs to be considered to enable H_2 transfer at mild conditions. Thus, no carbene system has been identified yet, that is able to activate and transfer H_2 in a similar way as it has been established since decades for the transition metals. To close this gap, the design of new tetrylenes with a specifically designed substitution pattern is required. However, the ability of silylenes/germylenes to activate H_2 is difficult to predict and still not fully understood. Therefore, optimizations of the H_2 activation by carbene species still relies on tedious trial-and-error experiments by varying the substitution pattern based on chemical intuition.

Similar to the substitution pattern in tetrylene chemistry, the choice of ligands in transition metal complexes is decisive for their ability to function as homogeneous catalysts. To accelerate catalyst design, the quantification of the steric and electronic ligand properties has early been

addressed first by experimental[8,9] and later by computational methods.[10] Based on this featurization of ligands improved ligand and catalyst structures can nowadays be predicted using computational and machine learning methods and has led to remarkable advances in the past few years.[11,12] While this approach has been widely used not only in transition metal and organocatalysis, but also in materials chemistry and drug design,[13] a similar strategy has not yet been applied for the specific design of main group species.[14] We envisioned that the field of main group element catalysis could also benefit from such an approach and the computer-aided selection and prediction of improved structures. To realize this goal, we aimed at the development of a model that allows to computationally describe and predict the propensity of tetrylenes to activate dihydrogen.

Here, we demonstrate that carbene systems can indeed be modelled like transition metal complexes and can be described by similar features as used in ligand design. This strategy allowed us to predict the activation energy for the H_2 activation with high accuracy based on the substituent properties and correlate the energy profiles of different tetrylenes (silylenes and germylenes) with each other. These results allow for a further understanding of the substituent properties crucial for bond activations and may be employed to accelerate the design of future main group compounds for small molecule activations.

Results and Discussion

Definition of the chemical space region and data generation. To explore the chemical space of heavier carbenes applicable in hydrogen activation, we conducted a virtual screening of compounds of type RER' with E = Si and Ge. We decided to focus our studies on silylenes and germylenes which we expected to be the most promising candidates for reversible H_2 activation due to the higher stability of the +2 oxidation state compared to carbenes combined with the higher activity and R-E bond strengths relative to the tin and lead analogues.[7] Initially, we focused on silylenes, which we generated in silico by combinatorial enumeration of different R substituents bound to the silicon center. To generate a large but also meaningful chemical space of silylenes, we initially chose substituents previously described in literature to form stable acyclic silylenes or germylenes, some of which were capable of activating dihydrogen (Figure 1),[5,6,15] and enlarged the library by derivatives of these substituents. This selection was made to ensure synthetic accessibility of the calculated systems. Overall, 40 substituents of different sizes and with different donor atoms (Figure 2) were used, including amido, alkyl and aryl, oxylato, thiolato, phosphanyl, silyl, *N*-heterocyclic iminyl (NHI) and boryl groups. Next, the silylenes were virtually generated from combinations of these substituents and thus used in further studies.

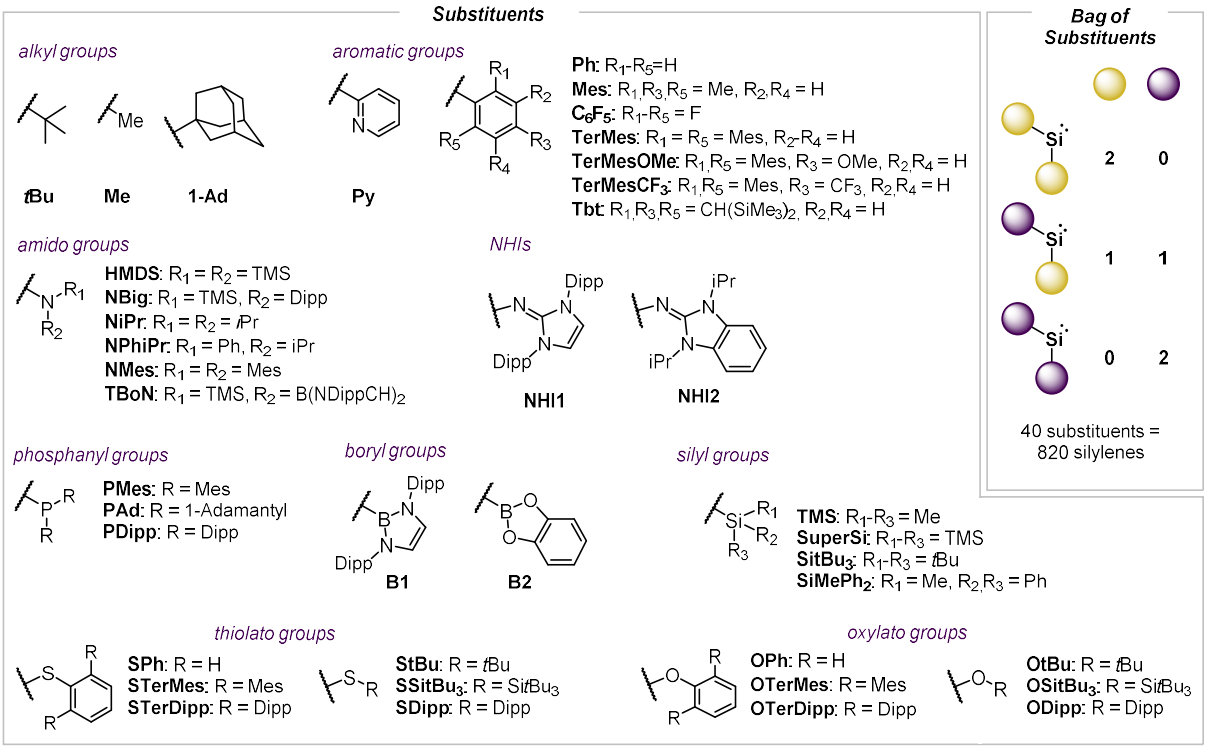

Figure 2. Substituent space with 40 substituents containing amido, aryl, oxylato, thiolato, alkyl, phosphanyl, silyl, NHI and boryl substituents.

Computational exploration of the reaction energies. For each of the obtained 598 silylenes the energy of the activation barrier **R¹R²Si-TS**, the activation product **R¹R²Si-H₂** and the silylene itself **R¹R²Si:** were calculated (Scheme 1, for detailed information see the Supporting Information). These energies were obtained through an automated procedure depicted in Figure 3. The initial geometry guesses for the silylenes and the H_2 activation products were generated from the corresponding SMILES strings via an initial geometry optimization at the GFN2-xTB level of theory with the GBSA solvent model for THF,[16] followed by a subsequent conformer ensemble generation using CREST at the same level of theory.[17] The lowest energy conformer was then chosen for further optimization at density functional theory (DFT) level (PBE0-D3/df2-svp//PBE0-D3/df2tzvp). For the transition states, the first structure guess was made based on the assumption that **R¹R²Si-TS** resembles the structure of the silylene **R¹R²Si:**. Starting from the optimized silylene structure the initial geometry guess for the transition state was obtained by addition of two hydrogen atoms to **R¹R²Si:** using mean distances, angles and dihedrals obtained from initially calculated transition states. As there are two possible locations for hydrogen atoms at both sides of the silylene, both TS were optimized on DFT level, from which the energetically favored TS was used in the following.

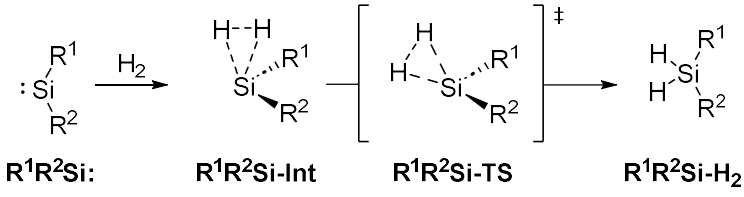

Scheme 1. Calculated mechanism for the dihydrogen activation at the silicon atom in silylenes. All energy values are given in Table S6, S7 and S8 in the Supporting Information.

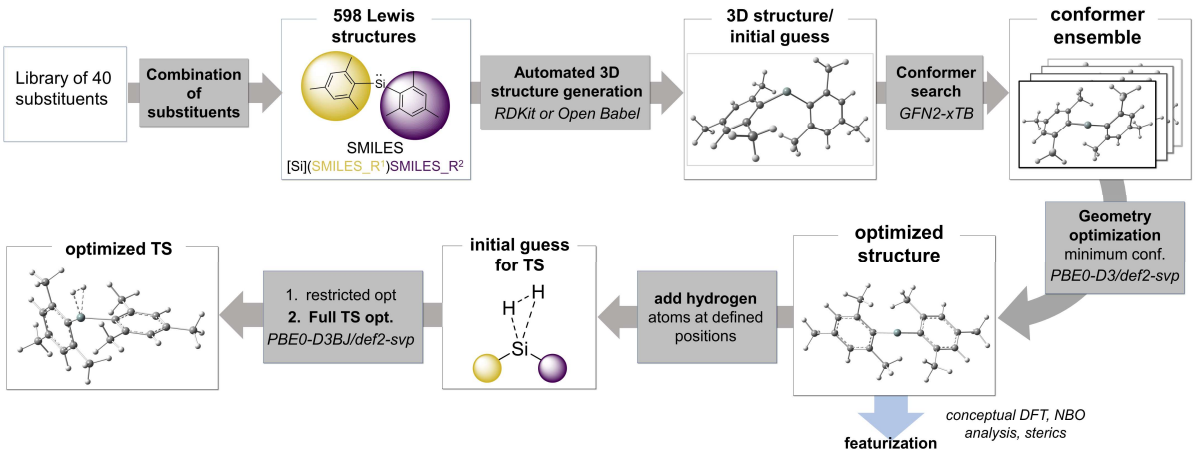

Figure 3. Workflow used to generate the DFT data used in this study.

It should be noted that during TS search two different modes of hydrogen activation were observed for some structures: the single-site and cooperative H_2 activation across the Si-R linkage.[18] These cooperative H_2 activations were mainly found for silylenes with boryl substituents due to the availability of an empty p-orbital at boron, but also for some silyl substituents. Within this work we decided to focus only on single-site H_2 activations, and thus tried to obtain only this transition state for each silylene. Transition states which could not clearly be determined as single-site were excluded from the dataset. Furthermore, it must be noted that in some cases the value for the "barrier" (energy difference between **R^1R^2Si-TS** and **R^1R^2Si:**) is negative. This can be explained by the formation of intermediate **R^1R^2Si-Int** (Scheme 1), in which H_2 coordinates to the silicon center through an interaction of the σ-bond of H_2 and the vacant p-orbital of the silicon center analogous to σ-complexes in transition metal complexes. For highly reactive and instable silylenes, **R^1R^2Si-Int** as well as **R^1R^2Si-TS** are energetically favored compared to the free silylene and H_2. In these cases, the energy difference is not equal to the actual barrier of the reaction, but still reflects the impact of the substituent on H_2 activation relative to the silylene. Thus, and for clarity, we used the term "barrier" in the following for all energy differences between the free silylene and the H_2 activation transition state.

Substituent increments for the activation and reaction energy. With the energy profiles of the H_2 activation for 598 silylenes at hand, we became interested in deducing systematic patterns between the substituents and the resulting energies, that would allow for a facile prediction of the activation potential of new silylenes. Based on the Benson group theory in thermochemistry,[19] we hypothesized that the calculated reaction energies and activation barriers for the hydrogen activation can be expressed as a sum of contributions from each substituent bound at the silicon center. This procedure was chosen in analogy to the "Bag of Substituents" first used by Tolman and recently by Gensch et al. to describe the properties of phosphine ligands in transition metal catalysis based on the sum of their substituent contributions.[20,21] To verify our hypothesis, we described all silylenes as a matrix of all unique substituents, with each matrix element expressing how often (0, 1, 2) a substituent is present in the silylene. Multivariate linear regression (Ridge) with a train-test-split of 70:30 led to a highly predictive model (Figure 4A), which confirmed the additivity of the substituent energies increments as reflected in the high quality coefficients of determination. For example, in case

of the activation energy a mean absolute error (MAE) of only 9.1 kJ/mol for the test set (R^2_{test} = 0.95) was determined. Additionally, we analyzed, how often a substituent must be present in the training data to obtain good results from the fit. Obviously, each substituent must be represented at least once in the training data, but slightly better results are obtained if each ligand is represented at least twice (for details see SI, Figure S7). Thus, models with larger proportion of the test set in the train-test-split still perform well. The prediction quality of the model for the reaction energy ΔG_{H2} was likewise very good (Figure 4B), and sufficiently accurate, so that we concluded that $\Delta G^{‡}$ and ΔG_{H2} of the H_2 activation can be expressed simply by the sum of their substituent increments.

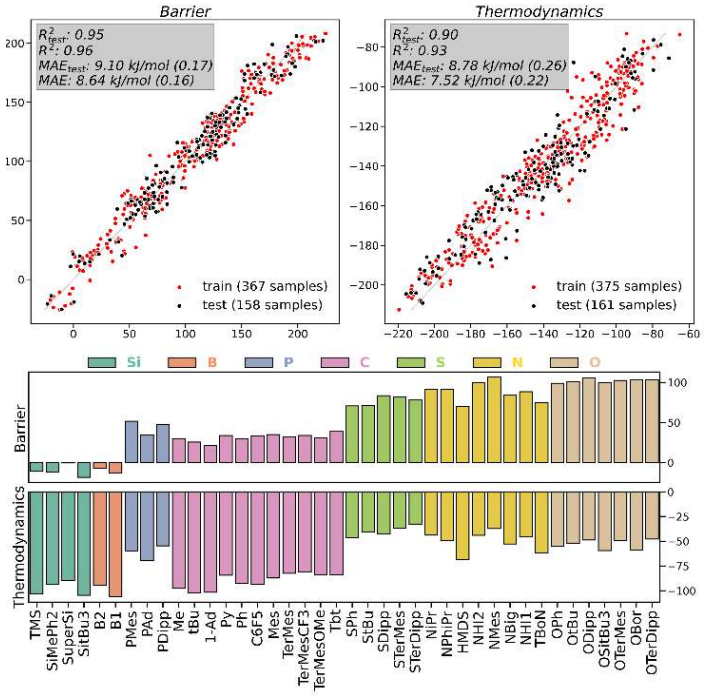

Figure 4. Performance of the ridge regression (train-test-split = 70:30) for the calculated and predicted (A) activation barrier and (B) reaction energy based on the Bag of substituents (Figure 1); Gibbs Free Energies ΔG in kJ/mol, x-axis: calculated ΔG, y-axis: predicted ΔG, MAE: mean absolute error in kJ/mol and relative to standard deviation. (C) Calculated barrier (top) and thermochemistry (bottom) increments in kJ/mol for all 40 substituents. Bars are coloured by the element of the substituents directly bound to the silicon center.

The final increments for all 40 substituents were obtained from the fit by the substituent coefficient and intercept. The bar plot of increments (Figure 4C) colored by the elements in α-position to the silicon center shows a strong dependence between the increment and this element. All substituents within each group have similar increments thus allowing for a rough estimation of the impact of a specific substituent on the activity of silylenes towards hydrogen. For example, boryl and silyl groups in general lead to low activation barriers – in line with the silylenes hitherto known to activate H_2 (Figure1) – but highly stable products from which H_2 elimination or transfer will be challenging to realize. On the other hand, N- and O-substituents lead to the reverse trend, i.e. high activation barriers and less exergonic reaction profiles, suggesting that a combination of these substituents with boryl or silyl groups might be better suited for realizing catalytic turn-over at mild conditions. Interestingly, phosphanyl substituents – such as those studied experimentally by Izod and coworkers for germylenes[22] – occupy an intermediate position suggesting a so far untapped potential of these silylenes in small

molecule activation.[23] Of all the substituents studied, they most likely would lead to a possible H_2 transfer judged based on the required energy for the back reaction. Nonetheless, a truly reversibly hydrogenation reaction will not be possible with these (or any other) substituents. However, this does of course not exclude hydrogenation reactions of unsaturated compounds such as alkenes, carbonyl compounds or imines, for which hydrogen transfer has a different activation barrier than the dehydrogenation reaction studied here.

Correlation of substituent properties with the activation energy and energy prediction. Thus far, the high-throughput virtual screening enabled a first computational exploration of the chemical space of silylenes for H_2 activation and demonstrated that the reaction energy and activation barrier can be predicted by substituent energy increments. However, the available data set also allows for an analysis of relationships between these energy values and the steric and electronic properties of the silylenes and their substituents. Given that the bag of substituents does not allow to predict energies of substituents beyond the used data set, such a correlation with physicochemical features would remove this limitation and facilitate extrapolation to so far untested substituents, which will be helpful to accelerate the exploration of potential main-group element catalysts in the future.

To describe the silylenes and their substituents and to guarantee interpretability of the results we selected a descriptor-based parametrization of the molecules including steric and electronic properties (Table S2+S3).[10] Such descriptors have been used for the featurization of ligands in transition metal catalysts and successfully applied for the prediction of optimal ligand structures to improve the catalytic performance.[11] A total of 98 features were obtained from DFT calculations, population analyses and conceptual DFT methods to characterize each silylene and the respective substituents (see the Supporting Information for details). The Pearson correlation coefficients were calculated to examine the correlation of the properties with the activation barrier and reaction energy (Figure 5). The HOMO-LUMO gap is often used in literature to explain the reactivity of carbenes towards small molecule activation.[4] Indeed, this descriptor was found to strongly correlate (ρ = 0.80) with the activation barrier, although the hardness of the silicon atom (= fundamental gap, IP-EA) showed a stronger correlation (ρ = 0.82) and thus would be better suited as a single descriptor for estimating the H_2 activation potential of silylenes.

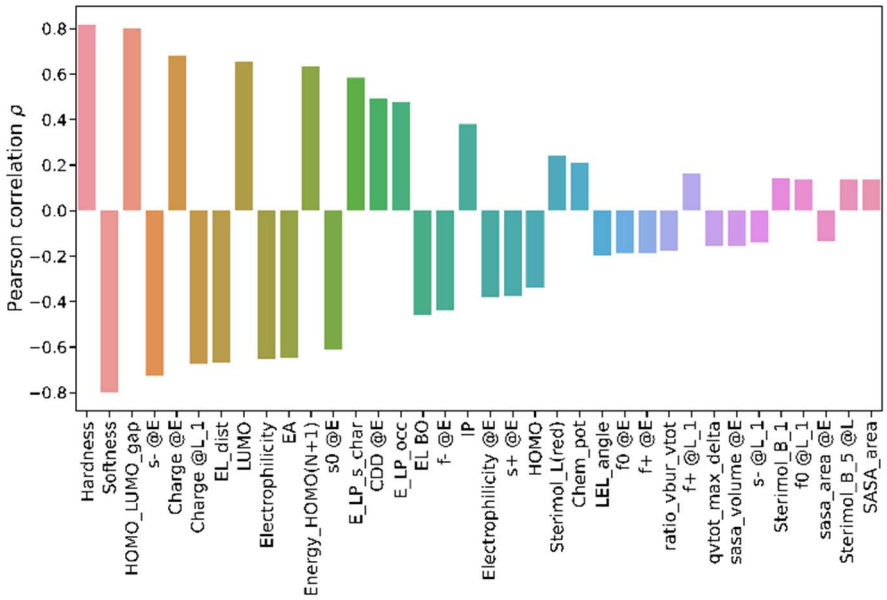

Figure 5. Pearson correlation ρ of calculated features with activation barrier.

Despite the strong correlation of both features with the barrier, using these features alone for univariate linear regression turned out to be insufficient for making reliable predictions of the activation energy. For example, regression of the HOMO-LUMO gap with the barrier results in a mean absolute error (MAE) of 25.8 kJ/mol (0.48) (R^2 = 0.64, Figure 6A). This limitation may be explained by the fact that the HOMO and LUMO orbitals are usually not entirely localized at the silicon center but often delocalized across the substituents. Another frequently discussed feature is the R1–Si–R2 angle, which however exhibits no correlation with the barrier according to our data (RER angle: R^2 = 0.04, MAE = 42.70 kJ/mol (0.79)). Consequently, this feature is not suitable for predicting barriers in acyclic silylenes, but may help to explain the higher barriers observed in cyclic silylenes compared to acyclic ones. To obtain a more reliable prediction of the H_2 activation barrier based on the silylenes properties, multivariate linear regression with 7 linear independent descriptors was performed, which enabled an improved prediction (MAE_{test} = 12.17 kJ/mol (0.22), Figure S12). Within this model, the HOMO-LUMO gap, the local softness s^- of the silicon atom in terms of the removal of an electron and the occupation of the lone pair at the silicon center are the most important features.

To both, simplify and further improve our model, we probed including a categorical variable for the elements in α-position to the silicon center in addition to the physicochemical descriptors, since we had observed a strong relationship between these elements and the calculated energy increments of the substituents (Figure 4). Similar to the bag of substituents, the categorical variable of elements in α-position was transformed into a matrix with all unique elements (Si, B, P, C, S, N, O) and the matrix elements describing how often this element is present in α-position (0, 1, 2) in the respective silylene. This approach again enabled the calculation of energy increments specific to these elements (Table 1). To our delight, this simple approach allowed for a fast estimation of the activation barrier, with a mean average error of only approx. 11 kJ/mol (R^2(test) = 0.95; see Figure S15). It is surprising that this model performs even better than the first model based on steric and electronic descriptors and underlines the importance of the nature of the α-element for the silylene properties. This simple model allows the rapid estimation of the activation barrier for any silylene based on the elements in the α-position and can therefore be easily calculated in head. For example, a barrier of about 64 k/mol (±11 kJ/mol) is expected for a diarylsilylene.

Table 1. Energy increments of barrier and thermodynamics in kJ/mol specific to the α-position of the silicon center.

Element in α-position	Increment for the activation barrier [kJ/mol]	Increments for reaction energy [kJ/mol]
Si	-9.38	-97.83
B	-9.87	-100.13
P	43.51	-63.17
C	31.69	-90.48
S	76.04	-39.89
N	86.21	-51.08
O	100.24	-53.71

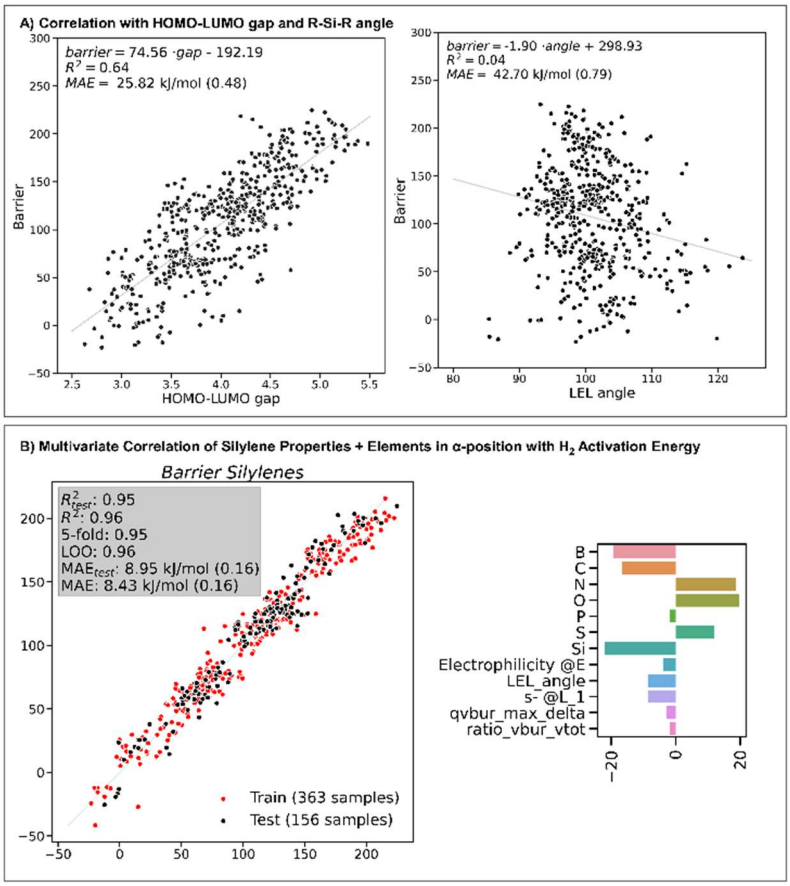

Figure 6. (A) Univariate correlation of the HOMO-LUMO gap and the RSiR' angle with the H_2 activation barrier and (B) Ridge regression of the element increments in combination with physiochemical properties with the activation barrier and display of the coefficients for the increments and properties (LOO = Leave-one-out). A description to all features used in the model is given in the Supporting Information.

Combining the matrix of the elements in α-position with five linearly independent property descriptors obtained from DFT calculations finally led to a model with ridge regression that predicts the barrier with a mean absolute error lower than 9 kJ/mol (MAE_{test} = 8.95 kJ/mol) and thus allows for a reliable prediction (Figure 6B). Within this model, the value of the R-Si-R angle, the softness of one of the substituents towards removal of an electron and the electrophilicity of the silicon atom were found to be the most important property features. Using the same approach for modelling the energy of the activation processes, also allowed for an accurate prediction of ΔG_{H2} with a MAE of only approx. 8 kJ/mol (Figure S22).

Predictions beyond the data set. Having established an accurate model, we next aimed at evaluating its predictive power. To this end, we investigated the hydrogen activation by the four new silylenes **1**-**4** (Figure 7). We intentionally opted for silylenes with phosphanyl groups, since they have so far little been investigated in silylene chemistry,[22] but revealed to be promising substituents for room temperature H_2 activation based on their energy increments (Figure 5). We chose substituents, which were not included in the original data set to probe the extrapolation capability of the model, with silylene **4** even consisting of two unknown substituents. To our delight, the predicted barriers were found to match the calculated barriers excellently, with an average deviation of only approx. 3 kJ/mol, thus confirming the predictive power of our model and the possible extrapolation to substituents unseen by the model. The

extremely small deviation from the calculated values is impressive, particularly when keeping in mind that only three phosphanyl substituents were included in the original chemical space, showing that this number is sufficient for the model to learn the decisive properties.
Based on the properties of the silylenes, compound **4** was predicted to exhibit the lowest barrier to activate dihydrogen. With a required activation barrier of only 106 kJ/mol, this silylene should be capable of activating dihydrogen at or close to room temperature. All other silylenes **1**-**3** also showed barriers lower than 125 kJ/mol indicating a possible activation at slightly elevated temperatures.

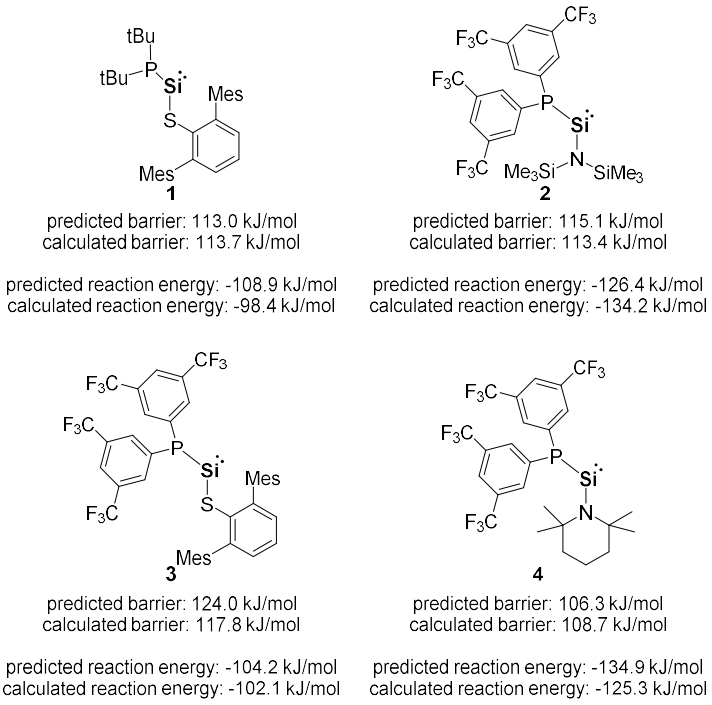

Figure 7. Structures of novel silylenes and their predicted and calculated activation barrier and reaction energy for hydrogen activation.

Energy prediction of the H_2 activation with germylenes. Having established relationships between the substituents in silylenes and their ability to activate H_2 as well as a predictive model based on substituent properties, we next became interested in transferring these results to the heavier analogue, the germylenes. Applying a similar procedure for the bag of substituents as described above on a smaller set of germylenes (23 substituents, 198 germylenes) confirmed the additivity of the substituent energy increments for determining the activation barrier and reaction energy (energy values are given in Table S5).
In order to establish a quantitative relationship between the different heavier carbenes, we examined whether the energy profile for the H_2 activation with germylenes can be predicted based on the silylene energies. Regression of the silylene and germylene activation energies indeed yielded a linear relationship expressed by equation 1 (Figure 8), which allows the prediction of the H_2 activation barrier for germylenes with an accuracy higher than 6 kJ/mol. The relationship demonstrates that H_2 activation with germylenes requires more energy than the activation with silylenes as expected due to the increasing stability of the +2 oxidation state of germanium. This stabilization can now be quantified. For a process which requires 100 kJ/mol with a silylene – i.e. which is just possible at room temperature – the predicted energy for the corresponding germylene is approx. 150 kJ/mol and thus requires elevated

temperature. The reverse trend is seen in the reaction energies. Here, hydrogen activation with a germylene is at least 100 kJ/mol less exergonic (eq. 2).

Barrier: $\Delta G^{\ddagger}(Ge) = 38.26\ kJ/mol + 1.10 \cdot \Delta G^{\ddagger}(Si)$ (eq. 1)

Reaction energy: $\Delta G(Ge) = 101.46\ kJ/mol + 1.17 \cdot \Delta G(Si)$ (eq. 2)

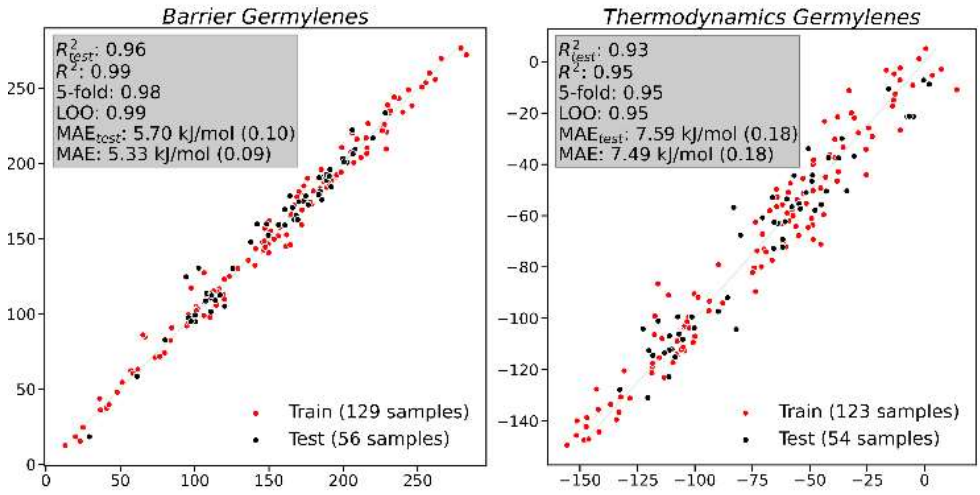

Figure 8. Performance of the correlation of the calculated (x axis) and predicted (y axis) activation and reaction energies for H_2 activation by acyclic germylenes with those of silylenes.

Conclusion

In summary, we have developed a computational model to predict the energy and activation barrier for the activation of dihydrogen at the group 14 element centers in silylenes and germylenes. Establishment of an automated workflow allowed the investigation of approx. 600 silylenes with 40 different substituents. The contribution of each substituent to the reaction and activation energy was found to be additive, allowing for the prediction of the energy values based on simple substituent energy increments. Surprisingly, even energy increments solely based on the elements in α-position to silicon enabled a prediction of the energy profile and thus represents a simple tool for estimating the reaction barrier in head. An accurate prediction of the activation and reaction energies with a mean error of less than 9 kJ/mol is possible via a multivariate linear regression with physicochemical properties of the silylenes in combination with energy increments for the elements in α-position to silicon. Evaluation of the predictive power of this model showed that also the H_2 activation propensity of silylenes with substituents not included in the original data set can be reliably predicted, which thus will accelerate the prediction of new silylene structures capable of H_2 activation in the future. The same procedure was applied to germylenes and furthermore their reactivity predicted based on the energy profile of the corresponding silylenes.

Overall, the presented study provides important guidelines for the design of carbene species for small molecule activation. The strong dependence of the activation and reaction energy on the nature of the element in α-position to the low-valent main group element allows for a simple and fast estimation of the energy profile and the prediction of new candidate structures. The

possible transfer of our model from one element to the other can presumably also be extended to other neutral and even charged carbene-like species, which will be important for evaluating the potential of other main group compounds in bond activation processes.

Computational Details

Detail about the density functional theory calculations and machine learning procedures including all calculated energies are given in the Supporting Information.

Acknowledgements

This work was supported by RESOLV, funded by the Deutsche Forschungsgemeinschaft (DFG, German Research Foundation) under Germany's Excellence Strategy – EXC-2033 - Projektnummer 390677874 and within the priority program SPP 2363.

References

[1] a) P. P. Power, Nature 2010, 463, 171; b) C. Weetman, S. Inoue, *Chem. Cat. Chem.* **2018**, *10*, 4213-4228; c) T. Chu, G. I. Nikonov, *Chem. Rev.* **2018**, *118*, 3608-3680; d) T. J. Hadlington, M. Driess, C. Jones, *Chem. Soc. Rev*. **2018**, *47*, 4176-4197.

[2] D. Martin, M. Soleilhavoup, G. Bertrand, *Chem. Sci*., **2011**, *2*, 389-399.

[3] G. D. Frey, V. Lavallo, B. Donnadieu, W. W. Schoeller, G. Bertrand, *Science* **2007**, *316*, 439-441

[4] a) M. Driess, *Nat. Chem.* **2012**, *4*, 525-526; b) D. Bourissou, O. Guerret, F. P. Gabbaï, G. Bertrand, *Chem. Rev.* **2000**, *100*, 39-92; c) Y. Mizuhata, T. Sasamori, N. Tokitoh, *Chem. Rev.* **2009**, *109*, 3479-3511; d) M. Usher, A. V. Protchenko, A. Rit, J. Campos, E. L. Kolychev, R. Tirfoin, S. Aldridge, *Chem. Eur. J.* **2016**, *22*, 11685-11698; e) S. Fujimori, S. Inoue, *Eur. J. Inorg. Chem.* **2020**, *2020*, 3131-3142; f) Y. Wang, J. Ma, *J. Organomet. Chem.* **2009**, *694*, 2567-2575.

[5] Silylenes capable of H2 activation: a) A. V. Protchenko, K. H. Birjkumar, D. Dange, A. D. Schwarz, D. Vidovic, C. Jones, N. Kaltsoyannis, P. Mountford, S. Aldridge, *J. Am. Chem. Soc*. **2012**, *134*, 6500-6503; b) A. V. Protchenko, A. D. Schwarz, M. P. Blake, C. Jones, N. Kaltsoyannis, P. Mountford, S. Aldridge, *Angew. Chem. Int. Ed.* **2012**, *52*, 568-571; c) D. Wendel, D. Reiter, A. Porzelt, P. J. Altmann, S. Inoue, B. Rieger, *J. Am. Chem. Soc.* **2017**, *139*, 17193-17198; d) D. Reiter, R. Holzner, A. Porzelt, P. J. Altmann, P. Frisch, S. Inoue, *J. Am. Chem. Soc.* **2019**, *141*, 13536-13546; e) C. Ganesamoorthy, J. Schoening, C. Wölper, L. Song, P. R. Schreiner, S. Schulz, *Nat. Chem.* **2020**, *12*, 608-614.

[6] Silylenes inactive towards H2: a) T. J. Hadlington, J. A. B. Abdalla, R. Tirfoin, S. Aldridge, C. Jones, *Chem. Commun*. **2016**, *52*, 1717-1720; b) B. D. Rekken, T. M. Brown, J. C. Fettinger, H. M. Tuononen, P. P. Power, *J. Am. Chem. Soc*. **2012**, *134*, 6504-6507; c) N. Weyer, M. Heinz, J. I. Schweizer, C. Bruh, M. C. Holthausen, U. Siemeling, *Angew. Chem. Int. Ed.* **2021**, *60*, 2624-2628; d) B. D. Rekken, T. M. Brown, J. C. Fettinger, F. Lips, H. M. Tuononen, R. H. Herber, P. P. Power, *J. Am. Chem. Soc.* **2013**, *135*, 10134-10148.

[7] Y. Peng, J. -D. Guo, B. D. Ellis, Z. Zhu, J. c. Fettinger, S. Nagase, P. P. Power, *J. Am. Chem. Soc.* **2009**, *31*, 16272–16282.

[8] C. A. Tolman, *Chem. Rev.* **1977**, *77*, 313–348.

[9] For examples: a) T. Allman, R. G. Goel, *Can. J. Chem.* **1982**, *60*, 716–722. b) H. V. Huynh, Y. Han, R. Jothibasu, J. A. Yang, Organometallics **2009**, *28*, 5395−5404; c) O. Back, M. Henry-Ellinger, C. D. Martin, D. Martin, G. Bertrand, *Angew. Chem., Int. Ed.* **2013**, *52*, 2939–2943; d) A. El-Hellani, J. Monot, S. Tang, R. Guillot, C. Bour, V. Gandon, *Inorg. Chem.* **2013**, *52*, 11493–11502; e) A. B. P. Lever, *Inorg. Chem.* **1991**, *30*, 1980−1985; f) A. R. Chianese, X. Li, M. C. Janzen, J. W. Faller, R. H. Crabtree, *Organometallics*, **2003**, *22*, 1663-1667.

[10] D. J. Durand, N. Fey, *Chem. Rev.* **2019**, *119*, 6561-6594.

[11] For examples: a) J. P. Reid, M. S. Sigman, M. *Nature* **2019**, 571, 343–348. b) G. dos Passos Gomes, R. Pollice, A. Aspuru-Guzik, *Trends in Chemistry* **2021**, 3, 96–110; c) A. F. Zahrt, J. J. Henle, B. T. Rose, Y. Wang, W. T. Darrow, S. E. Denmark, *Science* **2019**, 363, 6424; d) S. Zhao, T. Gensch, B. Murray, Z. L. Niemeyer, M. S. Sigman, M. S. M. R. Biscoe, *Science*, **2018**, 362, 670–674; e) S. Lin, J. C. Fromer, Y. Ghosh, B. Hanna, M. Elanany, W. Xu, *Sci. Rep.* **2021**, *11*, 4534; f) J. F. Goebel, J. Löffler, Z. Zeng, J. Handelmann, A. Hermann, I. Rodstein, T. Gensch, V. H. Gessner, L. J. Gooßen, *Angew. Chem. Int. Ed.* **2023**, *62*, e202216160.

[12] For reviews: a) M. S. Sigman, K. C. Harper, E. N. Bess, A. Milo, *Acc. Chem. Res.* **2016**, 49, 1292–1301. b) C. B. Santiago, J.-Y. Guo, M. S. Sigman, *Chem. Sci.* **2018**, 9, 2398–2412; c) A. Nandy, C. Duan, M. G. Taylor, F. Liu, A. H. Steeves, H. J. Kulik. *Chem. Rev*. **2021**, *121*, 9927-10000

[13] For examples, see: a) J. HAchmann, R. Olivares-Amaya, S. Atahan-Evrenk, C. Amador-Bedolla, R. S. Sanchez-Carrera, A. Gold-Parker, L. Vogt, A. M. Brockway, A. Aspuru-Guzik, *J. Phys. Chem. Lett.* **2011**, *2*, 2241-2251; b) G. A. Baldivia-Berroeta, Z. B. Zaccardi, S. K. F. Pettit, S.-H. Ho, B. W. Palmer, M. J. Lutz, C. Rader, B. P. Hunter, N. K. Green, C. Barlow, C. Z. Wayment, D. J. Ludlow, P. Petersen, S. J. Smith, D. J. Michaelis, J. A. Johnson, *Adv. Mater.* **2022**, *34*, 2107900.

[14] For an example with FLP, see: S. Das, R. C. Turnell-Ritson, P. J. Dyson, C. Corminboeuf, *Angew. Chem. Int. Ed.* **2022**, *61*, e202208987.

[15] Examples of acyclic germylenes: a) D. H. Harris, M. F. Lappert, *J. Chem. Soc., Chem. Commun.* **1974**, 895-896; b) M. F. Lappert, M. J. Slade, J. L. Atwood, M. J. Zaworotko, *J. Chem. Soc., Chem. Commun.* **1980**, 621-622; c) W. A. Merrill, R. J. Wright, C. S. Stanciu, M. M. Olmstead, J. C. Fettinger, P. P. Power, *Inorg. Chem.* **2010**, *49*, 7097-7105; d) J. Li, A. Stasch, C. Schenk, C. Jones, *Dalton Trans.* **2011**, *40*¸10448-10456; e) T. J. Hadlington, M. Hermann, J. Li, G. Frenking, C. Jones, *Angew. Chem. Int. Ed.* **2013**, *52*, 10199-10203; f) E. W. Y. Wong, T. J. Hadlington, C. Jones, *Main Group Met. Chem.* **2013**, *36*, 133-136; g) T. J. Hadlington, M. Hermann, G. Frenking, C. Jones, *J. Am. Chem. Soc.* **2014**, *136*, 3028-3031; h) B. Cetinkaya, I. Gümrükçü, M. F. Lappert, J. L. Atwood, R. D. Rogers, M. J. Zaworotko, *J. Am. Chem. Soc.* **1980**, *102*, 2088-2089; i) M. Driess, S. Yao, M. Brym, C. van Wüllen, *Angew. Chem. Int. Ed.* **2006**, *45*, 4349-4352; j) R. A. Green, C. Moore, A. L. Rheingold, C. S. Weinert, *Inorg. Chem.* **2009**, *48*, 7510-7512; k) K. Izod, E. R. Clark, W. Clegg, R. W. Harrington, *Organometallics* **2012**, *31*, 246-255; l) P. Jutzi, H. Schmidt, B. Neumann, H.-G. Stammler, *Organometallics* **1996**, *15*, 741-746; m) L. Pu, N. J. Hardman, P. P. Power, *Organometallics* **2001**, *20*, 5105-5109; n) G. H. Spikes, Y. Peng, J. C. Fettinger, J. Steiner, P. P. Power, *Chem. Commun.* **2005**, 6041-6043; o) X. Wang, Z. Zhu, Y. Peng, H. Lei, J. C. Fettinger, P. P. Power, *J. Am. Chem. Soc.* **2009**, *131*, 6912-6913; p) L. Li, T. Fukawa, T. Matsuo, D. Hashizume, H. Fueno, K. Tanaka, K. Tamao, *Nature Chem.* **2012**, *4*, 361-365; q) B. D. Rekken, T. M. Brown, J. C. Fettinger, F. Lips, H. M. Tuononen, R. H. Herber, P. P. Power, *J. Am. Chem. Soc.* **2013**, *135*, 10134-10148; r) J. W. Dube, Z. D. Brown, C. A. Caputo, P. P. Power, P. J. Ragogna, *Chem. Commun.* **2014**, *50*, 1944-1946.

[16] C. Bannwarth, S. Ehlert, S. Grimme, *J. Chem. Theory Comput.* **2019**, *15*, 1652–1671.

[17] P. Pracht, F. Bohle, S. Grimme, *Phys. Chem. Chem. Phys.*, **2020**, *22*, 7169-7192.

[18] a) N. Kuriakose, K. Vanka, *Dalton Trans.* **2014**, *43*, 2194-2201; b) H. Steinert, J. Löffler, V.H. Gessner, *Eur. J. Inorg. Chem.* **2021**, *2021*, 5004-5013; c) L. Greb, F. Ebner, Y. Ginzburg, L. M. Sigmund, *Eur. J. Inorg. Chem.* **2020**, *2020*, 3030-3047.

[19] S. W. Benson, F. R. Cruickshank, D. M. Golden, G. R. Haugen, H. E. O'Neal, A. S. Rodgers, R. Shaw, R. Walsh, Chem. *Rev*. **1969**, *69*, 279−324.

[20] C. A. Tolman, *J. Am. Chem. Soc.* **1970**, *92*, 2953−2956.

[21] T. Gensch, G. dos Passos Gomes, P. Friederich, E. Peters, T. Gaudin, R. Pollice, K. Jorner, A. Nigam, M. Lindner-D'Addario, M. S. Sigman, A. Aspuru-Guzik, *J. Am. Chem. Soc.* **2022**, *144*, 1205-1217.

[22] a) K. Izod, D. G. Rayner, S. M. El-Hamruni, R. W. Harrington, U. Baisch, *Angew. Chem. Int. Ed.* **2014**, *53*, 3636-3640; b) K. Izod, M. Liu, P. Evans, C. Wills, C. M. Dixon, P. G. Waddell, M. R. Probert, *Angew. Chem. Int. Ed.* **2022**, *61,* e202208851; For other phosphanlygermylenes, see: c) M. Driess, R. Janoschek, H. Pritzkow, S. Rell, U. Winkler, *Angew. Chem. Int. Ed. Engl.* **1995**, *34*, 1614-1616; d) B. P. Johnson, S. Almst tter, F. Dielmann, M. Bodensteiner, M. Scheer, *Z. Anorg. Allg. Chem*. **2010**, *636*, 1275–1285.

[23] P. Vermeeren, M. T. Doppert, F. M. Bickelhaupt, T. A. Hamlin, *Chem. Eur. J.* **2021**, *12*, 4526.